

The microstrip Silicon magnetic spectrometer of the PAMELA experiment

The PAMELA collaboration

Abstract

The PAMELA magnetic spectrometer is composed of a permanent magnetic system and six detector planes. Each detector plane consists of six double sided microstrip Silicon sensors glued together to obtain a useful area of $14 \times 16 \text{ cm}^2$ with a thickness of $300 \mu\text{m}$. The performances of the sensors were studied using both minimum and non minimum ionizing particles at the CERN (Geneva) and PSI (Zurich) facilities (Adriani, 1998). The measured spatial resolution and the main results of the tests are presented and their relevance for the PAMELA performances explained.

1 The PAMELA experiment

To study the antiparticles component in cosmic rays (CR) several experiments with balloons have been performed during the past years. Balloon-borne experiments are affected by the particles production in the residual atmosphere and by their short operational time, which limits the maximum measurable energy to $\sim 30 \text{ GeV}$. To improve our knowledge of the antiparticles spectra is recommendable to perform experiments outside the atmosphere.

The PAMELA experiment (The PAMELA collaboration, 1999) will be operational for at least three years on a polar orbit, at an altitude of 700 Km , thus allowing the measurement with large statistic of the CR flux over a wide energy range (from 100 MeV to $\sim 300 \text{ GeV}$). The main observational objective of the experiment is the measurement of the antiparticles flux (\bar{p} , e^+) and the search for antinuclei, with a sensitivity of better than 10^{-7} in the $\bar{\text{He}}/\text{He}$ ratio.

To perform these goals the PAMELA detector makes use of informations given by several subdetectors: a transition radiation detector (TRD), a magnetic spectrometer, an electromagnetic calorimeter and a system of scintillators for time of flight measurements (TOF). The TRD and the TOF give the particles velocity, that combined with the momentum, measured by the spectrometer, and the informations coming from the calorimeter, enables particles identification.

2 The magnetic spectrometer

The whole apparatus consists of a tracking system inserted into the cavity of a permanent magnet. Figure 1 shows a section of the spectrometer.

2.1 The magnet The magnet is composed of five modules, built in an alloy of Iron Neodymium and Boron, between which sensor planes are inserted. The total cavity volume available is $131 \times 161 \times 445 \text{ mm}^3$, resulting in a geometrical factor of $20.5 \text{ cm}^2\text{sr}$. Inside the cavity a mean magnetic field of 0.4 T is present. Outside the spectrometer the field is screened by a ferromagnetic shield.

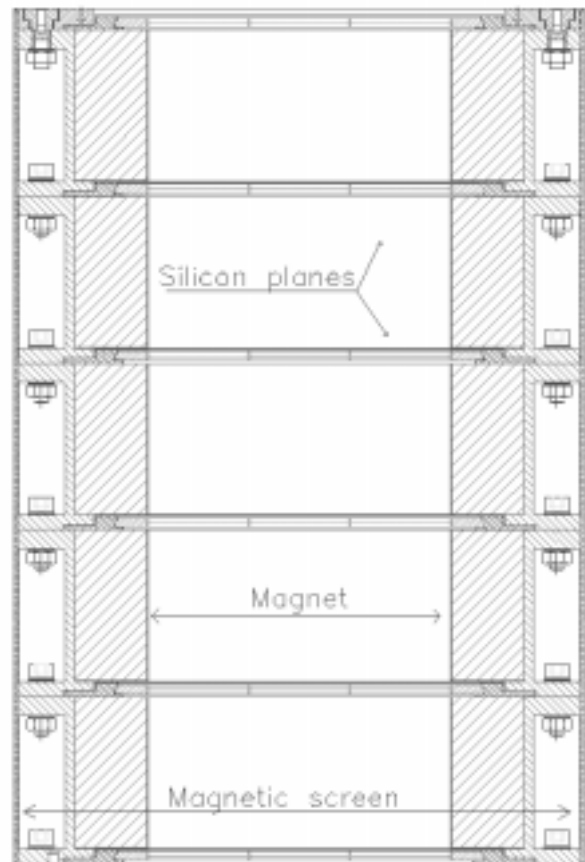


Figure 1: Section of the magnetic spectrometer; the total length is 44.5 cm .

2.2 The Silicon tracker The tracking system consists of six equally spaced planes of Silicon detectors, each composed by three ladders. The ladder is the basic detecting unit and is obtained by glueing together two Silicon sensors, 70 mm long, and an aluminium oxide hybrid, 55 mm long, that contains the front-end electronics (see figure 2). No additional material is present above or below the sensors in order to reduce multiple scattering.

- The Silicon sensors.** The detectors for the tracker are realized using double sided double metal AC coupled Silicon sensors. Each sensor consists of a high resistivity n-type Silicon wafer, 300 μm thick, with p^+ -type implanted strips on the junction side (strip pich of 25 μm) and n^+ -type implanted strips on the ohmic side (strip pich of 67 μm), with geometrical dimensions of $53.3 \times 70.0 \text{ mm}^2$. The strips on the ohmic side are implanted perpendicularly to those on the junction side and are separated by p^+ -type blocking strips. The decoupling capacitors, for signal running from the wafer to the electronics, are directly integrated on the Silicon sensors by separating the implanted strips from the readout metal strips by means of an insulating layer of Silicon dioxide. The insulating layer thickness is $100 \div 200 \text{ nm}$, resulting in a decoupling capacitance greater than 20 pF/cm. On the ohmic side a second metal layer is implanted in order to make the readout lines (readout pich of 50 μm) parallel on both sides. The ohmic contact between the two layers is realized by means of an etching procedure. As it is shown in figure 2, the contact is not univocal, but this ambiguity will be removed during the off-line analysis using the informations coming from the other detectors. The resulting detector is extremely compact and gives two independent coordinates of the traversing particle impact point, thus minimizing multiple scattering. The strips on the junction side will be used to measure the coordinate in the bending view (X view), to have the better spatial resolution.

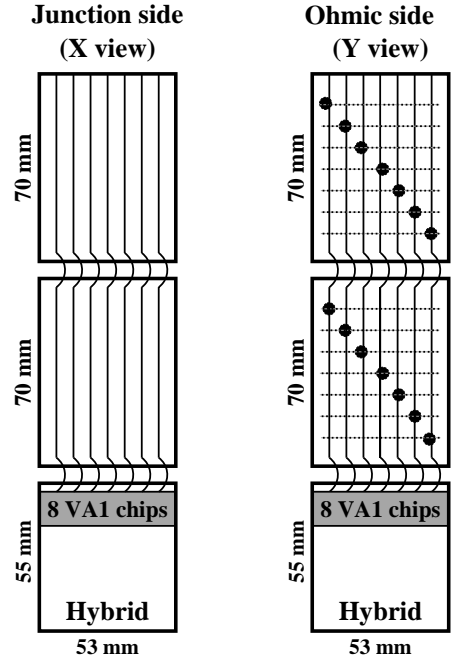


Figure 2: Schematic drawing of both sides of a ladder. The vertical lines are the readout strips. The horizontal dashed lines are the n^+ -type implanted strips on ohmic side and dots represent the ohmic contacts between the two layers.

- Frontend and Analog to Digital Conversion.** Since the spatial resolution of the detector is strongly correlated to its signal to noise ratio (S/N), the use of low-noise frontend electronics is of great importance. For that reason a VLSI chip, called VA1, has been selected for the frontend section. The VA1 chip consists of 128 charge sensitive preamplifiers each connected to a CR-RC shaper ($\sim 1 \mu\text{s}$ shaping time) and followed by a sample and hold circuitry. The outputs are multiplexed and the analog information is driven by a differential output buffer to the ADCs, that are placed on electronic boards housed immediately outside the magnetic screen. The digital data coming from the 12 bit ADCs are then transferred to the data acquisition system, where a Digital Signal Processor (DSP), after a preliminary analysis, compresses them to be stored in the memory.

3 Magnetic spectrometer performances

The tasks of the magnetic spectrometer are the measurement of the momentum of charged particles traversing the detector and the determination of the sign and the absolute value of their electric charge.

An important parameter to characterize the spectrometer performance is the maximum detectable rigidity (MDR), that is defined as the rigidity value for which the error on momentum measurement is equal to 100%. For given magnetic field intensity and spectrometer geometrical characteristics, the MDR is inversely propor-

tional to the spatial resolution of the tracker. For PAMELA, assuming a spatial resolution of $4 \mu\text{m}$, a MDR of 800 GV/c is obtained.

For the cosmic antiparticles flux determination the maximum measurable energy is not given by the spectrometer limits (i.e. MDR), but by the spillover effect. This effect comes from the wrong determination of the charge sign of the traversing particles due to the multiple scattering inside the spectrometer combined with the finite spatial resolution of the Silicon detectors. The effect is greatest for high values of the momentum and decreases by improving the spatial resolution of the tracker. Being antiparticles only a small fraction of CR, the particles spillover gives rise, at high energies, to a non negligible background. The spectrometer simulation shows that the p, e^- spillover sets a maximum energy limit in the \bar{p}, e^+ measurements to $\sim 200 \text{ GeV}$.

4 Test beam

During last years several tests have been performed, in order to evaluate the achievable spatial resolution and the S/N. The last one has been performed during September '98 at the PS accelerator at CERN.

4.1 Setup A telescope of four ladders, 6.7 cm apart from each other, was mounted in an aluminium box provided with a thin aluminium foil entrance and an exit window for the beam; the system was completed by two scintillators put at the beginning and at the end of the telescope, which were used for triggering. Only one of the four ladders was equipped with both sensors as foreseen in the project, the remaining three were equipped with only a single sensor. To test the apparatus a beam, composed mainly of π^- with energy of $\sim 3.5 \text{ GeV}$, was used.

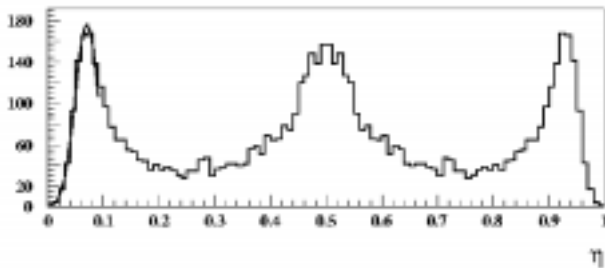


Figure 4: Symmetrized η -distribution for the X view of the double detector. The distribution shows three pronounced peaks. When the particle crosses the detector in a region around a readout strip, all the charge is collected by only one strip, whatever the impact point is. In this case η can be ~ 0 or ~ 1 (see definition 1), giving rise to the lateral peaks. The central peak is due to the presence of implanted strips that are not read; when the particle crosses the detector in a region around one of these strips the charge is equally shared between the two nearby read strips, so that $\eta \sim 0.5$.

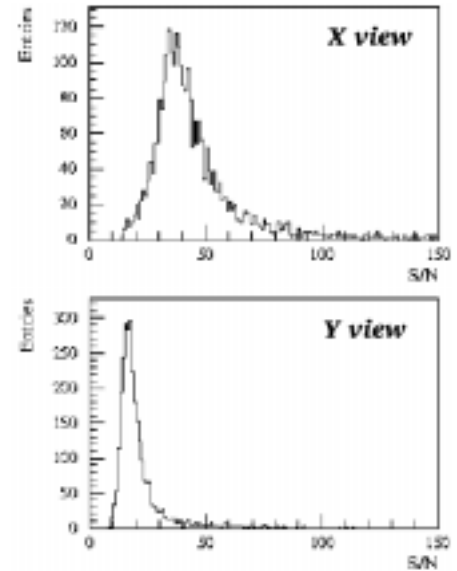


Figure 3: Signal to noise ratio distributions for the junction and ohmic side of the double detector, for minimum ionizing particles.

4.2 Data analysis and results The detectors performance is characterized by the S/N. Figure 3 shows the S/N distributions obtained for the two sides of the double detector; the mean values of the distributions are 45 and 21, respectively for the junction side and the ohmic side.

The spatial resolution is a fundamental parameter for the PAMELA apparatus because, as mentioned in section 3, it determines the maximum measurable energy of the CR spectrum. In the determination of the spatial resolution particular care is needed in the definition of the position finding algorithm (Turchetta, R., 1993), which has to take into account the charge spread over the strips; to obtain the best spatial resolution we have to use different algorithms, depending upon the incidence angle of the particles, the multiplicity of the cluster, and so on.

The simplest case is an incidence angle of 0° with respect to the normal to the sensor plane. In this case the informations related to the charge spread are con-

tained in the η -distribution. The η variable is defined as

$$\eta = \frac{S_R}{S_R + S_L}, \quad (1)$$

where, considering the two strips with the greatest signal in the cluster, $S_{R(L)}$ is the signal on the right (left) one and is related to charge partition between the strips. The η -distribution is the distribution of the η variable obtained when the detector is uniformly illuminated (see figure 4). The η -distribution enables to define a "non-linear on η algorithm" that directly takes into account the non linear sharing of the charge between strips. As an example, if the charge sharing was linear, the η -distribution would be flat and the algorithm would reduce to a "linear on η algorithm", that coincides with the centre of gravity of the two strips.

The spatial resolution measurement has been performed considering all the events for which a signal is released over three nearby planes, and computing the positional residuals distribution for the intermediate plane. The spatial resolution is obtained from the width of this distribution. Having only a double detector, two different configurations are used; with the three single ladders placed adjacently and with the double ladder placed between two single ladders. From the first configuration we obtain the spatial resolution of the single detector; given this value, from the second configuration we obtain the spatial resolution of the double detector. Figure 5 shows the positional residual distribution for the double detector fitted with a gaussian curve. From the standard deviation resulting from the gaussian fit we obtain the values for the spatial resolution quoted in the table.

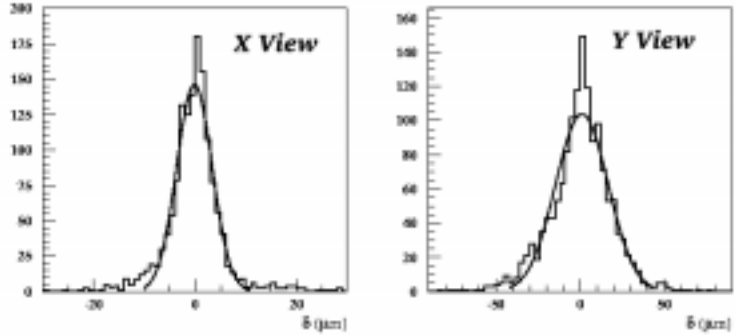


Figure 5: *Positional residuals distribution for the X and Y view of the double detector.*

view	Spatial resolution (μm)
X	3.0 ± 0.1
Y	11.5 ± 0.6

The choice of the "non-linear on η algorithm", according to literature, has given the best results.

5 Conclusions

To improve spatial resolution a careful study of the charge spread over the strips, which depends on detector geometry and signal to noise performance, is necessary. All the informations coming from the analysis of non inclined tracks will be used to implement proper position finding algorithms for inclined tracks within a magnetic field, which will be the real operational condition of the PAMELA detector.

References

- The PAMELA Collaboration 1999, Proc. 26th ICRC (Salt Lake City), OG.4.2.04
 Adriani, O., et al. 1998, Nucl. Instr. Meth. A409, 447
 Turchetta, R., 1993, NIM A335, 44